Geomechanics and Engineering, *Vol. 21, No. 6 (2020) 527-536*
DOI: https://doi.org/10.12989/gae.2020.21.6.527

Undrained solution for cavity expansion in strength degradation and tresca soils

Chao Li[a], Jin-feng Zou[b] and Yu-ming Sheng*

School of Civil Engineering, Central South University, Hunan 410075, China

(Received May 5, 2019, Revised March 28, 2020, Accepted May 16, 2020)

Abstract. An elastic-plastic solution for cavity expansion problem considering strength degradation, undrained condition and initial anisotropic in-situ stress is established based on the Tresca yield criterion and cavity expansion theory. Assumptions of large-strain for plastic region and small-strain for elastic region are adopted, respectively. The initial in-situ stress state of natural soil mass may be anisotropic caused by consolidation history, and the strength degradation of soil mass is caused by structural damage of soil mass in the process of loading analysis (cavity expansion process). Finally, the published solutions are conducted to verify the suitability of this elastic-plastic solution, and the parametric studies are investigated in order to the significance of this study for in-situ soil test.

Keywords: Tresca yield criterion; cavity expansion; elastic-plastic solution; strength degradation; undrained condition; initial anisotropic in-situ stress; large-strain

1. Introduction

Since the cavity expansion theory (CET) was applied into the analysis of foundation engineering in 1970s (Vesic, 1972), and the cavity expansion theory has been widely used in the field of geotechnical engineering, including in-situ soil test, tunnel excavation, anchor and the bearing capacity of pile foundation, etc. This theory (CET) was investigated by considering different stress state, consolidation history of soil mass and boundary conditions, such as the following aspects: theoretical analysis (Vesic 1972, Collins and Yu 1996, Yu and Rowe 1999, Wang *et al.* 2012a, Wang *et al.* 2012b, Mo *et al.* 2014, Xiao and Liu 2016a, Xiao *et al.* 2016b, Li *et al.* 2017, Mo and Yu 2017, Zou *et al.* 2017, Zou and Xia 2017, Pan *et al.* 2018, Sivasithamparam and Castro 2018, Zhou *et al.* 2018, Li *et al.* 2019, Li and Zou 2019, Sivasithamparam and Castro 2020, Zhang and Li, 2020); engineering problem (Vesic 1977, Randolph *et al.* 1979, Merifield *et al.* 2001, Manandhar and Yasufuku 2013, Castro *et al.* 2014, Wijewickreme and Weerasekara 2015, Zou *et al.* 2016, Khanmohammadi and Fakharian 2018, Kwon *et al.* 2018, Chen *et al.* 2019a, b, Qian *et al.* 2020); numerical analysis and in-situ soil test (Gibson and Anderson 1961, Teh and Houlsby 1991, Nash *et al.* 1992, Hight *et al.* 1992, Einav and Randolph 2005, Mo *et al.* 2017); and others.

For the cavity expansion analysis, it has already been well covered in the literature by a large number of researchers under the drained condition, e.g., Yu and Houlsby (1991) proposed a closed-form solution for cavity expansion problem in finite dilatant soil mass. Yu and Carter (2002) proposed a rigorous solution for created cavity (zero radii) problem in purely frictional and cohesive frictional soil mass based on the similarity solution techniques. Manandhar and Yasufuku proposed an analytical solution for the end-bearing capacity of tapered piles problem in purely frictional soil mass based on the spherical cavity expansion theory (Manandhar and Yasufuku 2012). Manandhar *et al.* (2012) proposed an analytical solution for the skin friction of tapered piles problem in sands based on the cavity expansion theory (Manandhar *et al.* 2012). Chen and Abousleiman (2013) proposed an exact drained solution for cylindrical cavity expansion problem in soft soils based on the modified Cam Clay model. Li *et al.* (2017) proposed a unified drained solution for spherical cavity expansion problem in clay and sand based on a critical state model, and so on. A drained cavity expansion analysis definitely will be more suitable for the interpretation of the soils with very high permeability. However, for the interpretation of the soft soils with very low permeability, an undrained cavity expansion analysis definitely will be more suitable.

However, most of the published papers for cavity expansion problem not taken into account the strength degradation behaviour of soil mass, these analyses not accord with field situation in practice, the strength degradation of soil mass is caused by structural damage of soil mass in the process of loading analysis (cavity expansion process) (Zou and Xia 2017), besides, most of the published papers for cavity expansion problem not taken into account the initial anisotropic in-situ stress of soil

*Corresponding author, Professor
E-mail: shengyuming_csu@163.com
[a]Ph.D.
E-mail: lichao@csu.edu.cn
[b]Professor
E-mail: zoujinfeng_csu@163.com

ISSN: 2005-307X (Print), 2092-6219 (Online)

mass, the assumption of isotropic condition was usually used in calculation to simplify the calculation, but, the initial in-situ stress may be anisotropic due to the influence of consolidation history of soil mass (Anderson 1980). Zou and Xia (2017) proposed a solution for cavity expansion problem in strain-softening soil mass based on the unified strength failure criterion, however, the initial stress state in the soil mass was not explicitly defined and only just referred to by an indirect parameter b. Although Pan *et al.* (2018) considered soil structure, it was also in isotropic soil mass, based on this, this paper will consider initial stress anisotropy and spherical expansion.

Comparing with other elasto-plastic models, the Tresca model is one of the most widely used models in the field of soil mechanics at present. Its main characteristics are: the clear basic concepts, better suited for geomaterials, as well as only one parameter (it can be easily obtained by conventional soil testing), which is easy to popularization in geotechnical engineering practice. At the same time, the initial in-situ stress state of natural soil mass may be anisotropy caused by consolidation history, and the strength degradation of soil mass caused by structural damage of soil mass in the process of load analysis (cavity expansion process). The main purpose of this paper is to study the influence of strength degradation and initial stress anisotropy on cavity expansion problem. In addition, the improvement and correction of its limitations based on the Tresca model is still an important direction for geotechnical material model, which needs further study.

Finally, this study is focus on undrained condition, initial anisotropic in-situ stress, the influence of strength degradation, and the Tresca yield criterion. The published solutions are conducted to verify the suitability of this solution, the parametric studies are investigated in order to the significance of this study for in-situ soil test.

2. Theory and methodology

2.1 Problem definition and assumptions

2.1.1 Problem definition

In Fig. 1, the cylindrical and spherical cavities are assumed to be initially subjected to an initial horizontal pressure $p_0(\sigma_{h0})$ (inner and exterior), an initial vertical stress σ_{v0} and an initial pore water pressure u_{w0}. The parameter K_0, which is equal to the ratio of the effective horizontal stress ($\sigma'_{h0}= \sigma_{h0}- u_{w0}$) and effective vertical stress ($\sigma'_{v0}= \sigma_{v0}- u_{w0}$), is used to reflect the initial anisotropic in-situ stress behaviour of soil mass. An initial radius of a_0 expands to a radius of a when the initial inner pressure is gradually increased from p_0 to p, which leads to an intermediate state as illustrated in Fig. 1. Upon loading, the cylindrical/spherical cavity first experiences elastic deformation and then plastic yielding when the yield condition is met at any point around the cavity, and a plastic region will then be formed from the current radius a to the elastic-plastic (EP) boundary r_b. The radial displacement of r_b is $U_{rb}=r_b- r_{b0}$.

2.1.2 Assumptions

Some assumptions are expressed as:

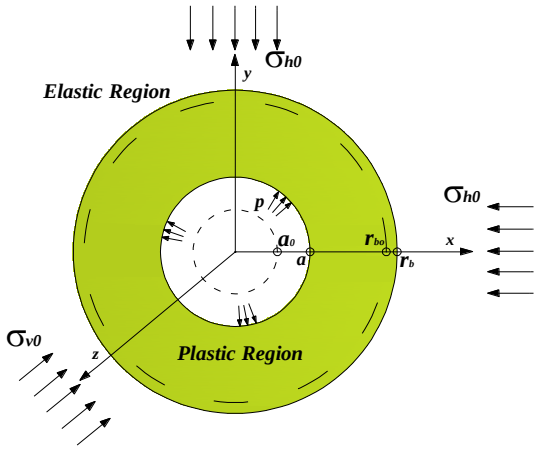

Fig. 1 The mechanism of cavity expansion

(1) For soil mass obeying the Tresca yield criterion, the radial and tangential stresses (σ_r and σ_θ) should obey the following yield criterion (Shuttle 2007):

$$2s_u = \sigma_r - \sigma_\theta \tag{1}$$

where s_u is the shear strength.

(2) For undrained saturated clay, the volumetric strain of soil mass is always zero in the process of cavity expansion, the change rate of the cavity boundary is uniform.

2.2 Elastic region ($r \geq r_b$)

In elastic region, the equilibrium equation is expressed as,

$$\begin{cases} k\dfrac{\sigma'_r-\sigma'_\theta}{r}+\dfrac{d\sigma'_r}{dr}+\dfrac{du_w}{dr}=0 \\ k\dfrac{\sigma_r-\sigma_\theta}{r}+\dfrac{d\sigma_r}{dr}=0 \end{cases} \tag{2}$$

where the parameter k are equal to 1 for a cylindrical cavity expansion and 2 for a spherical cavity expansion, the pore water pressure is u_w, σ'_r and σ'_θ are the effective radial and tangential stresses, respectively.

The stress and displacement of soil mass are expressed as follows in elastic region,

$$\sigma_r = (\sigma_{rb}-\sigma_{h0})\left(\frac{r_b}{r}\right)^{k+1}+\sigma_{h0} \tag{3}$$

$$\sigma_\theta = \sigma_{h0}-\frac{(\sigma_{rb}-\sigma_{h0})}{k}\left(\frac{r_b}{r}\right)^{k+1} \tag{4}$$

$$U=\frac{(1+\nu)(\sigma_{rb}-\sigma_{h0})r_b}{kE}\left(\frac{r_b}{r}\right)^k=\frac{(\sigma_{rb}-\sigma_{h0})r_b}{2kG}\left(\frac{r_b}{r}\right)^k \tag{5}$$

The boundary values are expressed as,

$$\sigma_r(r=a)=p \tag{6}$$

$$\sigma_r\left(r=r_b\right)=\sigma_{rb} \tag{7}$$

$$\lim_{r\to\infty}\sigma_r=\sigma_{h0} \tag{8}$$

The displacement of soil mass around the cavity is expressed,

$$U_{rb}=\frac{(1+\nu)(\sigma_{rb}-\sigma_{h0})r_b}{kE}=\frac{(\sigma_{rb}-\sigma_{h0})r_b}{2kG} \tag{9}$$

2.3 Elasto-plastic analysis ($a \le r \le r_b$)

Substituting the Tresca yield criterion (Eq. (1)) into the equilibrium equations (Eq. (2)), the equilibrium equation can also be expressed as,

$$k\frac{2s_u}{r}+\frac{d\sigma_r}{dr}=0 \tag{10}$$

$$U_{rb}=r_b-r_{b0}=\frac{(1+\nu)(\sigma_{rb}-\sigma_{h0})r_b}{kE}=\frac{(\sigma_{rb}-\sigma_{h0})r_b}{2kG} \tag{11}$$

For undrained condition, the volumetric strain vanishes. The following relation between the current and initial positions of a particle around the cavity (Fig. 1), r and r_0, and of the cavity wall, a and a_0 are given (Vesic 1972, Chen and Abousleiman 2012),

$$a^{k+1}-a_0^{k+1}=r^{k+1}-r_0^{k+1} \tag{12}$$

At EP boundary,

$$r_b^{k+1}-r_{b0}^{k+1}=r_b^{k+1}-\left(r_b-u_{rb}\right)^{k+1}=a^{k+1}-a_0^{k+1} \tag{13}$$

Following Collins and Yu (1996), the radial speed of the particle around the cavity can be expressed,

$$w=\dot{r}=\left(\frac{a}{r}\right)^k\dot{a} \tag{14}$$

So, the radial and tangential strain rates are expressed as,

$$\varepsilon_r=-\frac{dw}{dr}=\left(\frac{ka^k}{r^{k+1}}\right)\dot{a} \tag{15}$$

$$\varepsilon_\theta=-\frac{w}{r}=-\left(\frac{a^k}{r^{k+1}}\right)\dot{a} \tag{16}$$

The volumetric strain can be written as,

$$\varepsilon_p=\varepsilon_r+k\varepsilon_\theta \tag{17}$$

For undrained condition,

$$\varepsilon_r=-k\varepsilon_\theta \tag{18}$$

Corresponding to the deviator stress q (Cao *et al.* 2001), the shear strain can be expressed as,

$$\gamma=\frac{k}{\sqrt{3^k}}\left(\varepsilon_r-\varepsilon_\theta\right) \tag{19}$$

Combining Eqs. (18) and (13), the shear strain can also be expressed as,

$$\gamma=\frac{k}{\sqrt{3^k}}\ln\left(1-\frac{a^{k+1}-a_0^{k+1}}{r^{k+1}}\right) \tag{20}$$

The shear strength of soil mass is affected by structure of soil mass, and the following relationship is expressed as (Einav and Randolph, 2005),

$$s_u=s_{u0}\bullet\left(\delta_{rem}+\left(1-\delta_{rem}\right)e^{-3\xi/\xi_{95}}\right)\bullet\left(1+\mu\log\left(\left(\max\left(\left|\dot{\gamma}_{\max}\right|,\dot{\gamma}_{\max}^{0}\right)\right)\Big/\left(\dot{\gamma}_{\max}^{0}\right)\right)\right) \tag{21}$$

where s_{u0} is initial shear strength, ξ_{95} and δ_{rem} are the coefficient of strength degradation, δ_{rem} may be taken as the inverse of the sensitivity of soil mass, and ξ_{95} is the cumulative plastic shear strain of soil strength degradation to 95%, ξ is the cumulative plastic shear strain, μ is the coefficient of strain rate, and the value of μ changes from 0.05 to 0.2 (Einav and Randolph, 2005), $|\dot{\gamma}_{\max}|$ is the absolute value of maximum shear strain rate, $\dot{\gamma}_{\max}^{0}$ is the shear strain rate at reference point.

Combining Eqs. (12), (18) and (19), the shear strength of soil mass also is expressed as,

$$s_u(r)=s_{u0}\bullet\left(\delta_{rem}+(1-\delta_{rem})\exp\left(\frac{3k}{\xi_{95}\sqrt{3^k}}\ln\left(1-\left(a^{k+1}-a_0^{k+1}\right)/r^{k+1}\right)\right)\right)\bullet\left(1+\mu\log\left(\left(\frac{k(k+1)}{\sqrt{3^k}}\left(\frac{a^k}{r^{k+1}}\right)\dot{a}\right)\Big/\dot{\gamma}_{\max}^{0}\right)\right) \tag{22}$$

Combining Eqs. (11) and (13), the ratio of the radius of the plastic region (r_b) to the radius of cavity wall (a) can be given as follows,

$$\frac{r_b}{a}=\left(\frac{\left(\frac{a_0}{a}\right)^{k+1}-1}{\left(1-\frac{\sigma_{rb}-\sigma_{h0}}{2kG_0}\right)^{k+1}-1}\right)^{1/(k+1)} \tag{23}$$

At EP boundary, the stress of soil mass around the cavity can be expressed as (Chen *et al.* 2012),

$$\sigma'_{r0}=\sigma'_{\theta0}=\left(\sigma_{h0}-u_{w0}\right)=K_0\sigma'_{z0}=K_0\left(\sigma_{z(v)}-u_{w0}\right) \tag{24}$$

$$\frac{\sigma'_{r0}}{\sigma'_{h0}}=\frac{\sigma'_{\theta0}}{\sigma'_{h0}}=\frac{3K_0}{1+2K_0} \tag{25}$$

$$\frac{\sigma'_{z0}}{\sigma'_{h0}}=\frac{3}{1+2K_0} \tag{26}$$

The stress can also be derived by considering the EP boundary condition and the Tresca yield function,

$$\begin{aligned}\sigma_{rb}&=u_{w0}+\frac{3K_0}{1+2K_0}\sigma'_{h0}+s_{u0}\\&=u_{w0}+\frac{3K_0}{1+2K_0}\left(\sigma_{h0}-u_{w0}\right)+s_{u0}\end{aligned} \tag{27}$$

$$\sigma_{\theta b}=u_{w0}+\frac{3K_0}{1+2K_0}\left(\sigma_{h0}-u_{w0}\right)-s_{u0} \tag{28}$$

So,

$$\sigma_{rb}-\sigma_{h0}=\frac{K_0-1}{1+2K_0}\left(\sigma_{h0}-u_{w0}\right)+s_{u0} \tag{29}$$

$$\begin{aligned}\frac{r_b}{a}&=\left(\frac{\left(\frac{a_0}{a}\right)^{k+1}-1}{\left(1-\frac{\sigma_{rb}-\sigma_{h0}}{2kG_0}\right)^{k+1}-1}\right)^{1/k+1}\\&=\left(\frac{\left(\frac{a_0}{a}\right)^{k+1}-1}{\left(1-\frac{\frac{K_0-1}{1+2K_0}\left(\sigma_{h0}-u_{w0}\right)+s_{u0}}{2kG_0}\right)^{k+1}-1}\right)^{1/k+1}\end{aligned} \tag{30}$$

2.4 Total stresses

Based on the Eq. (27), the total stress distribution around the cavity in plastic region can be obtained,

$$\begin{aligned}\sigma_{rp}&=\sigma_a-\int_a^r\frac{2ks_u(r)}{r}dr\\&=u_{w0}+\frac{3K_0}{1+2K_0}\left(\sigma_{h0}-u_{w0}\right)+s_{u0}\\&\quad-2k\int_{r_b}^{a}\frac{\left(s_{u0}\cdot\left(\delta_{rem}+(1-\delta_{rem})\exp\left(\frac{3k}{\xi_{95}\sqrt{3^k}}\ln\left(1-\left(a^{k+1}-a_0^{k+1}\right)/r^{k+1}\right)\right)\right)\right)}{\cdot\left(1+\mu\log\left(\left(\frac{k(k+1)}{\sqrt{3^k}}\left(\frac{a^k}{r^{k+1}}\right)\dot{a}\right)\Big/\dot{\gamma}^0_{\max}\right)\right)}dr\\&\quad-\int_a^r\frac{2ks_u(r)}{r}dr\end{aligned} \tag{31}$$

$$\begin{aligned}\sigma_{\theta p}&=\sigma_a-\int_a^r\frac{2ks_u(r)}{r}dr\\&=u_{w0}+\frac{3K_0}{1+2K_0}\left(\sigma_{h0}-u_{w0}\right)+s_{u0}\\&\quad-2k\int_{r_b}^{a}\frac{\left(s_{u0}\cdot\left(\delta_{rem}+(1-\delta_{rem})\exp\left(\frac{3k}{\xi_{95}\sqrt{3^k}}\ln\left(1-\left(a^{k+1}-a_0^{k+1}\right)/r^{k+1}\right)\right)\right)\right)}{\cdot\left(1+\mu\log\left(\left(\frac{k(k+1)}{\sqrt{3^k}}\left(\frac{a^k}{r^{k+1}}\right)\dot{a}\right)\Big/\dot{\gamma}^0_{\max}\right)\right)}dr\\&\quad-\int_a^r\frac{2ks_u(r)}{r}dr-2s_u(r)\end{aligned} \tag{32}$$

2.5 Pore water pressure

For undrained condition, the volumetric strain of soil mass vanishes in the cavity expansion process. So, the change of p' is also zero. This means that the excess pore pressure (Δu_p) is equal to the change of the mean total stress. Therefore, the excess pore water pressure can be obtained as,

$$\begin{aligned}\Delta u_p&=\Delta p=u_{w0}+\frac{3K_0}{1+2K_0}\left(\sigma_{h0}-u_{w0}\right)+s_{u0}\\&\quad-2k\int_{r_b}^{a}\frac{\left(s_{u0}\cdot\left(\delta_{rem}+(1-\delta_{rem})\exp\left(\frac{3k}{\xi_{95}\sqrt{3^k}}\ln\left(1-\left(a^{k+1}-a_0^{k+1}\right)/r^{k+1}\right)\right)\right)\right)}{\cdot\left(1+\mu\log\left(\left(\frac{k(k+1)}{\sqrt{3^k}}\left(\frac{a^k}{r^{k+1}}\right)\dot{a}\right)\Big/\dot{\gamma}^0_{\max}\right)\right)}dr\\&\quad-\int_a^r\frac{2ks_u(r)}{r}dr-s_u(r)-p'_0\\&=u_{w0}+\frac{3K_0}{1+2K_0}\left(\sigma_{h0}-u_{w0}\right)+s_{u0}\\&\quad-2k\int_{r_b}^{a}\frac{\left(s_{u0}\cdot\left(\delta_{rem}+(1-\delta_{rem})\exp\left(\frac{3k}{\xi_{95}\sqrt{3^k}}\ln\left(1-\left(a^{k+1}-a_0^{k+1}\right)/r^{k+1}\right)\right)\right)\right)}{\cdot\left(1+\mu\log\left(\left(\frac{k(k+1)}{\sqrt{3^k}}\left(\frac{a^k}{r^{k+1}}\right)\dot{a}\right)\Big/\dot{\gamma}^0_{\max}\right)\right)}dr\\&\quad-\int_a^r\frac{2ks_u(r)}{r}dr-s_u(r)-\sigma'_{h0}\end{aligned} \tag{33}$$

3. Validation and parametric study

3.1 Validation

The solution of Shuttle (2007) also is conducted to verify the suitability of this study. The chosen parameters are (the parameters of Liu *et al.* (2017) can be used for reference), s_{u0}/σ'_{v0}=1.0, I_r=G/s_{u0}=100. The initial stress state is assumed to be isotropic (K_0=1). Shuttle (2007) proposed a cylindrical (k=1) elasto-plastic cavity expansion solution based on the Tresca yield criterion. In order to verify the correctness of this study, μ=0, δ_{rem}=1, namely, without considering the strain rate and strength degradation of soil mass. The results of the presented solution compared with the Shuttle's solution (2007) are shown in Fig. 2 and Fig. 3.

It can be seen from the Fig. 2 that the presented normalized cylindrical cavity pressure along the radial distribution is gradually equal to the Shuttle's solution without considering the strain rate and the strength degradation (μ=0, δ_{rem}=2). The difference may be that the hoop strain of Shuttle's paper (Shuttle, 2007) in the small-strain isotropic elastic region is expressed by the expression of large deformation analysis ε_θ=ln(r/r_0) (Chen and Abousleiman 2013), and substituting $\varepsilon_{r,yield}$=$s_u/2G$=1/2I_r=ln(r/r_0) into the Shuttle's equation of radius r, $r_s^2=\left(a^2-a_0^2\right)\Big/\left(1-e^{-\frac{1}{I_r}}\right)$. However, when K_0=1(isotropic condition), the radius of the presented

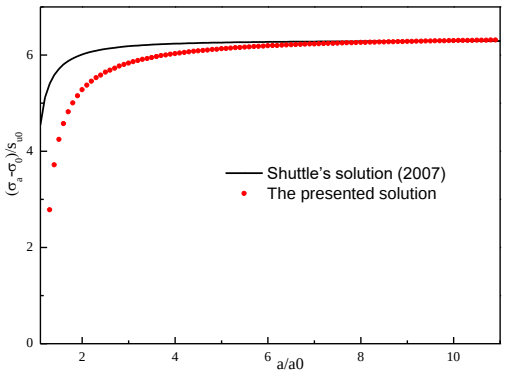

Fig. 2 The normalized cylindrical cavity pressure along the radial distribution

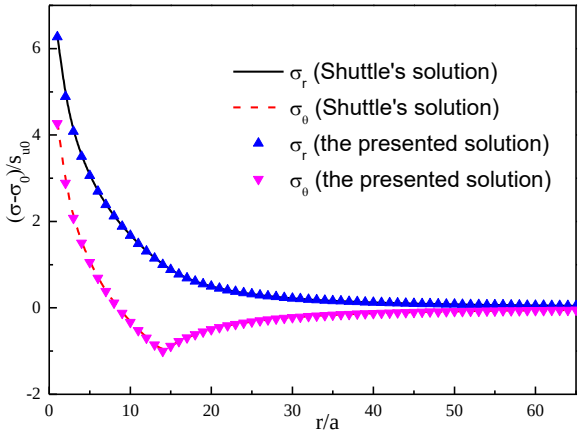

Fig. 3 The normalized radial and tangential stress along the radial distribution

solution is, $r^2_p=(a^2)\ r_p^2=\left(a^2-a_0^{\ 2}\right)\Big/\left(\left(1-s_u/2G\right)^2-1\right)$, and $e^x=1+x+\frac{1}{2!}x^2+\frac{1}{3!}x^3+\ldots$, so $r_p\neq r_s$. So the difference is generated.

It can be seen from the Fig. 3 that the presented normalized radial and tangential stress along the radial distribution is consistent with the Shuttle's solution without considering the strain rate and the strength degradation (μ=0, δ_{rem}=1), the rationality of this study is also verified.

3.2 Parametric study

To estimate the influences of the various parameters, the value of the parameters are taken from Einav and Randolph (2005) and Zhou and Randolph (2007), ξ_{95}=10~20, $\dot{\gamma}^0_{\max}=3\times10^{-6}\mathrm{s}^{-1}$, $\mu=0.05\sim0.2$, the field penetration rate is 20 mm/s. δ_{rem}=0~1. The other chosen parameters are s_{u0}/σ'_{v0}=1.0, $I_r=G/s_{u0}$=50~500, σ'_{v0}=100 kPa, a_0=0.1 m.

3.2.1 The influence of strength degradation

The parameter of initial stress state is assumed to be isotropic (K_0=1), $I_r=G/s_{u0}$=200, ξ_{95} and δ_{rem} are the coefficient of strength degradation, ξ_{95}=10~50, μ=0.1, δ_{rem}=0.5.

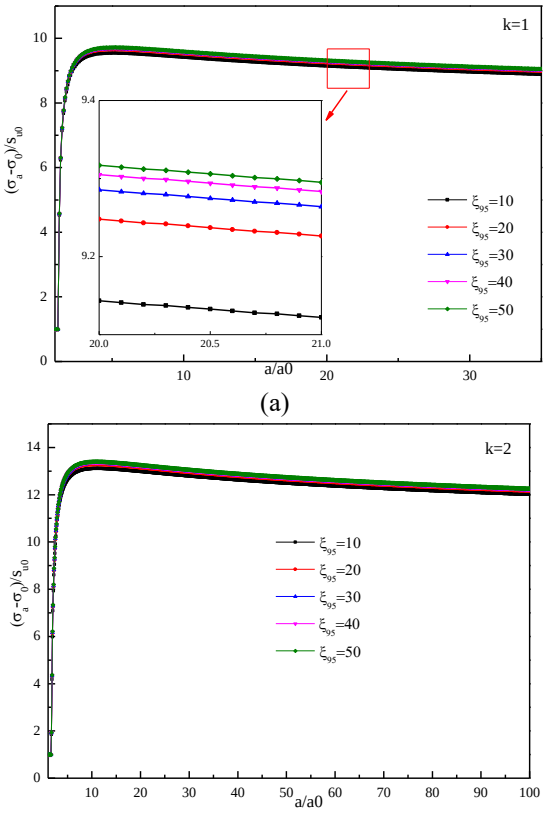

Fig. 4 The normalized cavity pressure with ξ_{95} along the radial distribution, (a) k=1 and (b) k=2

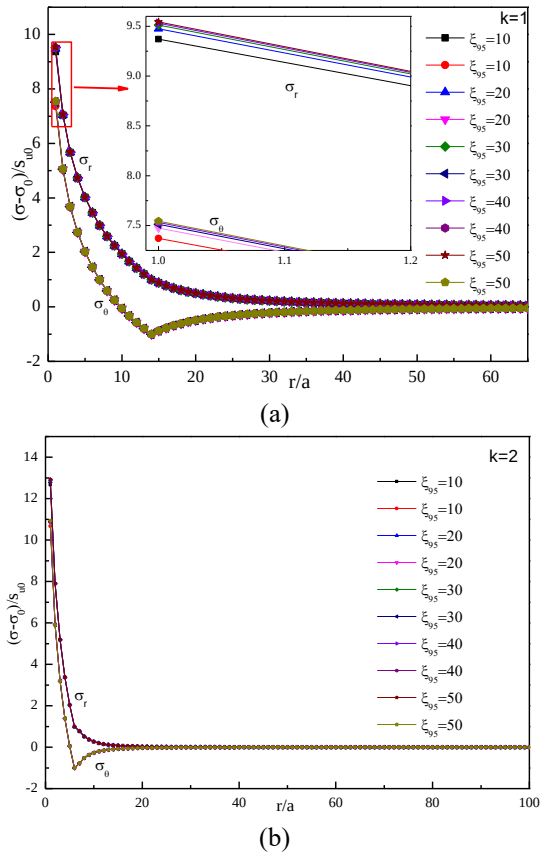

Fig. 5 The normalized radial and tangential stress with ξ_{95} along the radial distribution, (a) k=1 and (b) k=2

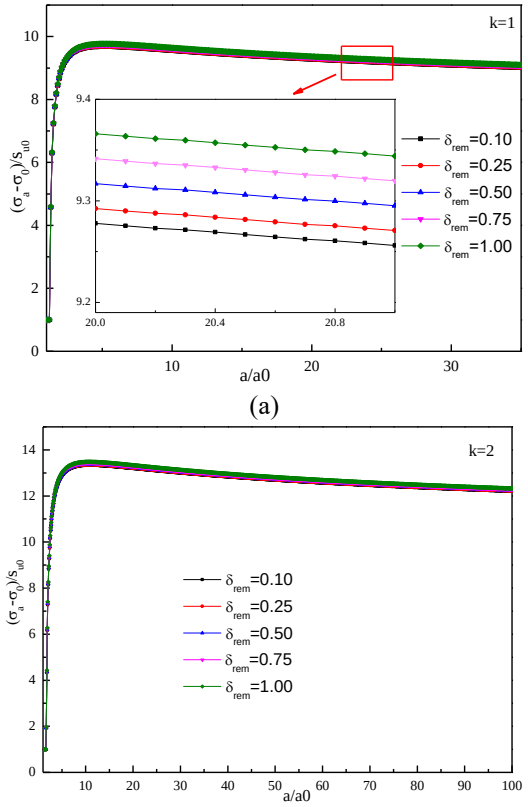

Fig. 6 The normalized cavity pressure with δ_{rem} along the radial distribution, (a) k=1 and (b) k=2

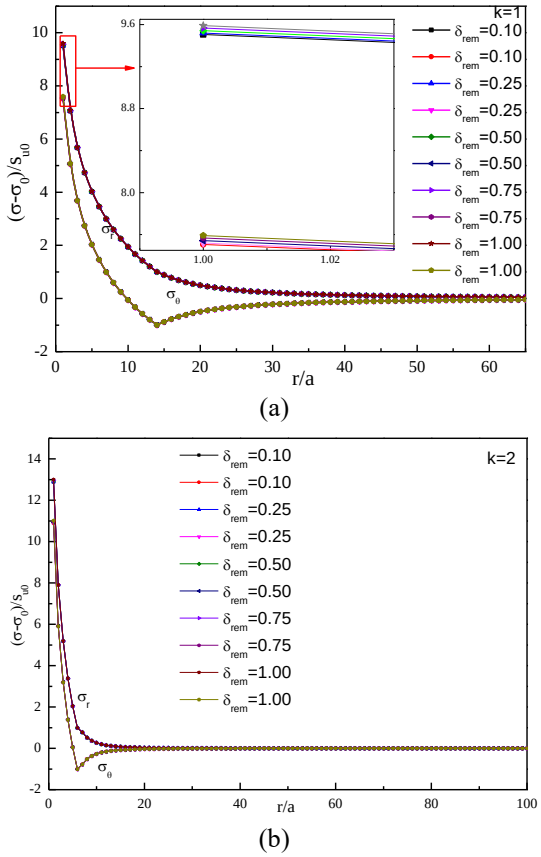

Fig. 7 The normalized radial and tangential stress with δ_{rem} along the radial distribution, (a) k=1 and (b) k=2

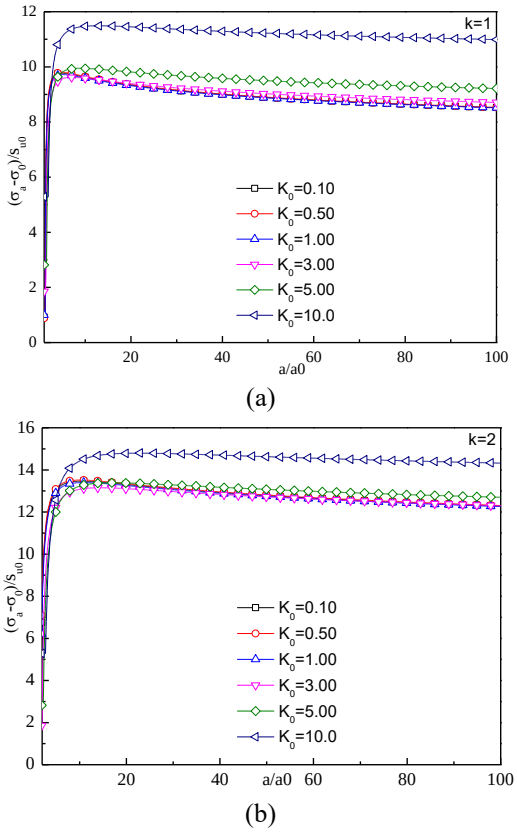

Fig. 8 The normalized cavity pressure with K_0 along the radial distribution, (a) k=1 and (b) k=2

The parameter of initial stress state is assumed to be isotropic (K_0=1), I_r=G/s_{u0}=200, ξ_{95} and δ_{rem} are the coefficient of strength degradation, ξ_{95}=50, δ_{rem}=0~1, μ=0.1.

As shown in Fig. 4 and Fig. 6, the influence of the parameter δ_{rem} on the normalized cavity pressure along the radial distribution is investigated for k=1 and k=2, the influence of the parameter δ_{rem} on the normalized cavity pressure is not obvious along the radial distribution. In local enlarged results of Fig. 4(a), it is worth noting that the normalized cavity pressure increases with ξ_{95} increasing from 10 to 50. The normalized cavity pressure first increases nonlinearly with the increase of the a/a0, and later decreases nonlinearly with the increase of the a/a0, reflecting the strength degradation property. As shown in Fig. 5 and Fig. 7. The influence of the parameter δ_{rem} on the normalized radial and tangential stress along the radial distribution are investigated for k=1 and k=2, the influence of the parameter δ_{rem} on the normalized radial and tangential stress is also not obvious along the radial distribution. In local enlarged results of Fig. 5(a), it also is worth noting that the normalized radial and tangential stresses increases with ξ_{95} increasing from 10 to 50. In local enlarged results of Fig. 6(a), it is worth noting that the normalized cavity pressure increases with δ_{rem} increasing from 0.1 to 1.0, and in local enlarged results of Fig. 7(a), it also is worth noting that the normalized radial and tangential stresses increases with δ_{rem} increasing from 0.1 to 1.0. To avoid duplication, similar local enlarged results have not been included in other figures.

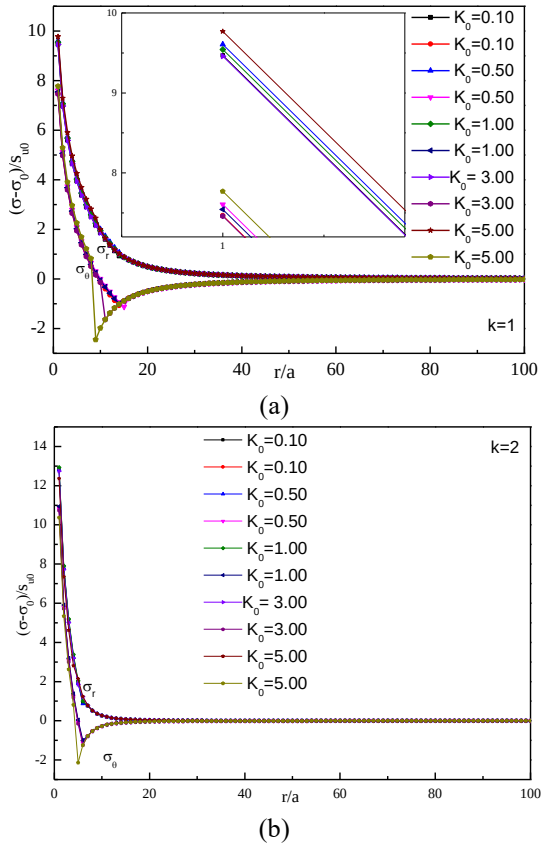

Fig. 9 The normalized radial and tangential stress with K_0 along the radial distribution, (a) k=1 and (b) k=2

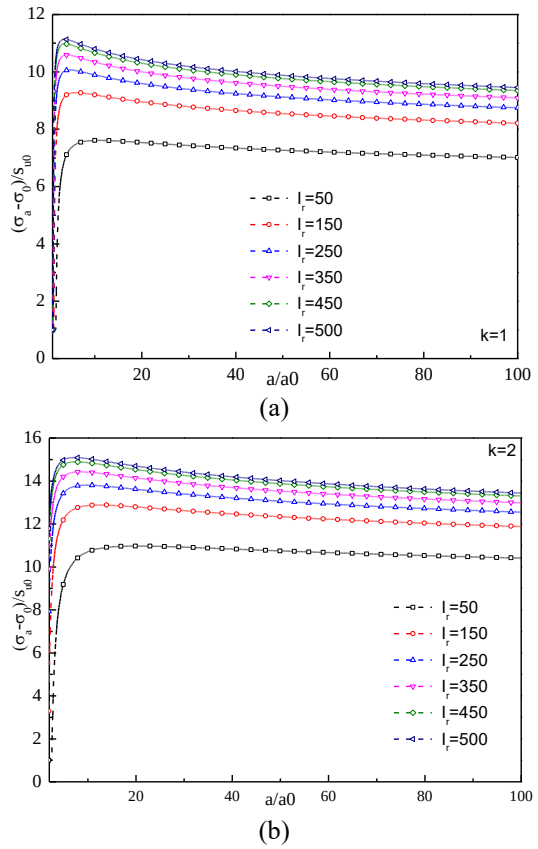

Fig. 10 The normalized cavity pressure with I_r along the radial distribution, (a) k=1 and (b) k=2

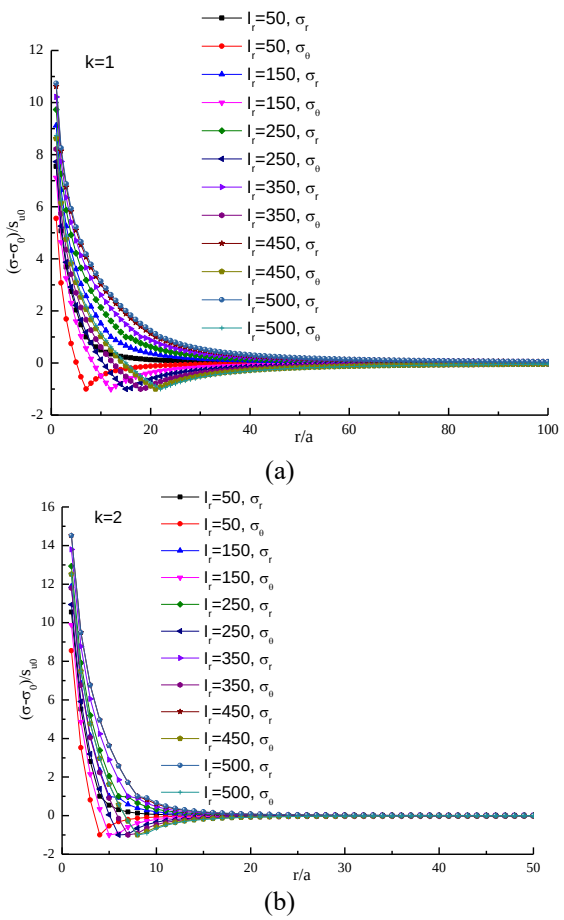

Fig. 11 The normalized radial and tangential stress with I_r along the radial distribution, (a) k=1 and (b) k=2

3.2.2 The influence of initial stress state

The parameter of initial stress state is assumed to be anisotropic ($K_0 \neq 1$), $I_r=G/s_{u0}=200$, $\delta_{rem}=0.5$, $\zeta_{95}=50$, $\mu=0.1$.

As shown in Fig. 8. The influence of the parameter K_0 on the normalized cavity pressure along the radial distribution is investigated for k=1 and k=2. The normalized cavity pressure increases with the increase of the parameter K_0. The normalized cavity pressure first increases nonlinearly with the increase of the a/a0, and later decreases nonlinearly with the increase of the a/a0, reflecting the strength degradation property. As shown in Fig. 9,the influence of the parameter K_0 on the normalized radial and tangential stress along the radial distribution are investigated for k=1 and k=2, the influence of the parameter K_0 on the normalized radial and tangential stress is also not obvious except the surrounding of elastic-plastic interface. However, in local enlarged results of Fig. 9(a), it also is worth noting that the normalized radial and tangential stresses increases with K_0 increasing from 0.1 to 5.0. The results imply that the value of the normalized radial and tangential stresses produced by the conventional solution (isotropic condition) is wrong for those obtained by the presented solution (anisotropic condition) in the same parameters, and the conventional solution will lead to an underestimation ($1.0 \leq K_0 \leq 5.0$) or overestimation ($0.1 \leq K_0 \leq 1.0$) of the normalized radial and tangential stresses and gives incorrect solution in engineering application, such as,

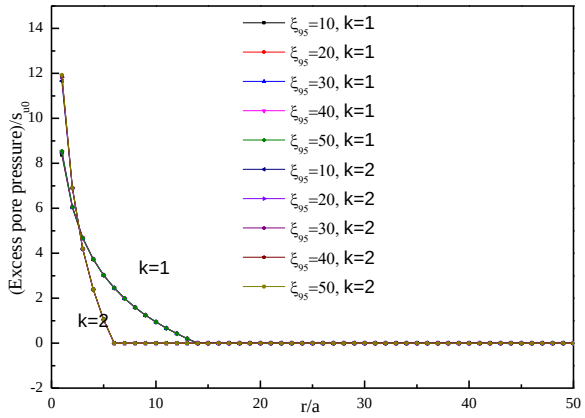

Fig. 12 The normalized excess pore water pressure with ξ_{95} along the radial distribution

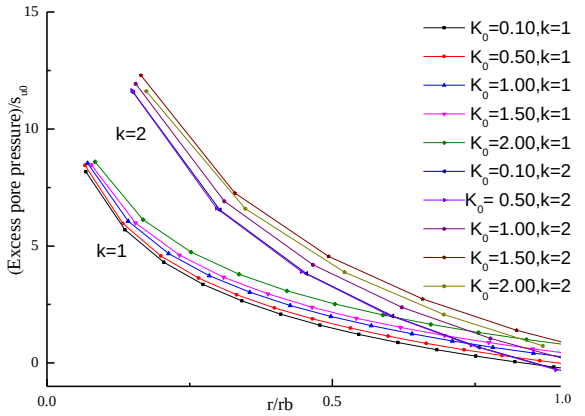

Fig. 13 The normalized excess pore water pressure with K_0 along the radial distribution

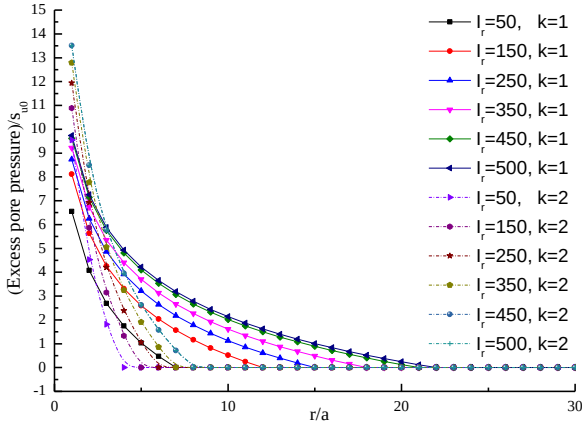

Fig. 14 The normalized excess pore water pressure with I_r along the radial distribution

in-situ soil test, tunnel excavation, anchor and the bearing capacity of pile foundation, etc.

3.2.3 The influence of the soil rigidity index

The parameter of initial stress state is assumed to be isotropic (K_0=1), I_r=G/s_{u0}=50~500, δ_{rem}=0.5, ξ_{95}=50, μ=0.1.

As shown in Fig. 10, the influence of the parameter I_r on the normalized cavity pressure along the radial distribution is investigated for k=1 and k=2. The normalized cavity pressure increases evidently with the increase of the parameter I_r. The normalized cavity pressure first increases nonlinearly with the increase of the a/a0, and later decreases with the increase of the a/a0, reflecting the strength degradation property. The strength degradation property is obvious with the increase of the parameter I_r. As shown in Fig. 11, the influence of the parameter I_r on the normalized radial and tangential stress along the radial distribution are investigated for k=1 and k=2, the influence of the parameter I_r on the normalized radial and tangential stress is also obvious in the plastic region with the increase of the parameter I_r.

3.2.4 Excess pore pressure

As shown in Fig. 12, the influence of the parameter ξ_{95} on the normalized excess pore water pressure along the radial distribution is also not obvious for k=1 and k=2. As shown in Fig. 13, the normalized excess pore water pressure in the plastic region increases evidently with the increase of the parameter K_0 ($0.1 \le K_0 \le 2$) for k=1 and k=2. As shown in Fig. 14, the influence of the parameter I_r on the normalized excess pore water pressure along the radial distribution is obvious for k=1 and k=2, the influence of the case (k=1) on normalized excess pore water pressure along the radial distribution is obvious than that the influence of the case (k=2) on normalized excess pore water pressure.

4. Conclusions

On the basis of the Tresca yield criterion and considering the influence of anisotropic initial stress state and strength degradation, the undrained elastic-plastic solution for cavity pressure, total stress distribution and excess pore pressure are described in this study. Compared with the previous solutions, the following improvements have been achieved:

(1) The undrained elastic-plastic solution eliminates the limitation of the condition of isotropic initial stress state which is usually required by existing results, so it can be applied to more general cases.

(2) Loading analysis, the undrained elastic-plastic solution considers the influence of strength degradation, which is usually neglected by existing results, so it can be applied into the structural damage of soil mass.

(3) The parametric analysis imply that the stress will be miscalculated if the strength degradation, rigidity index and stress anisotropy factor are ignored in natural soil mass. The normalized cavity pressure first increases nonlinearly with the increase of the a/a0, and later decreases nonlinearly with the increase of the a/a0, reflecting the strength degradation property; The influence of the parameter K_0 on the normalized radial and tangential stress is also not obvious except the surrounding of elastic-plastic interface; The normalized excess pore water pressure in the plastic region increases evidently with the increase of the parameter K_0 ($0.1 \le K_0 \le 2$) for k=1 and k=2. The influence of the case (k=1) on normalized excess pore water pressure along the radial distribution is obvious than that the influence of the case (k=2) on normalized excess pore water pressure.

Acknowledgments

This work was supported by the National Key R&D Program of China (2017YFB1201204). The first author thanks Project 2018zzts188 supported by Innovation Foundation for Postgraduate of the Central South University. The editor's and anonymous reviewer's comments have improved the quality of the study and are also greatly acknowledged.

References

Ahn, H.Y., Oh, D.W. and Lee, Y.J. (2018), "Behaviour of vertically and horizontally loaded pile and adjacent ground affected by tunneling", *Geomech. Eng.*, **15**(3), 861-868. https://doi.org/10.12989/gae.2018.15.3.861.

Andersen, K.H. (1980), "Cyclic and static laboratory tests on Drammen clay", *J. Geotech. Eng. Div.*, **106**(5), 499-529.

Cao, L.F., Teh, C.I. and Chang, M.F. (2001), "Undrained cavity expansion in modified cam clay I: Theoretical analysis", *Géotechnique*, **51**(4), 323-334. https://doi.org/10.1680/geot.2001.51.4.323.

Castro, J., Karstunen, M. and Sivasithamparam, N. (2014), "Influence of stone column installation on settlement reduction", *Comput. Geotech.*, **59**(3), 87-97. https://doi.org/10.1016/j.compgeo.2014.03.003.

Chen, G.H., Zou, J.F. and Chen, J.Q. (2019a), "Shallow tunnel face stability considering pore water pressure in non-homogeneous and anisotropic soils", *Comput. Geotech.*, **116**, 103205. https://doi.org/10.1016/j.compgeo.2019.103205.

Chen, G.H., Zou, J.F., Min, Q., Guo, W.J. and Zhang, T.Z. (2019b), "Face stability analysis of a shallow square tunnel in non-homogeneous soils", *Comput. Geotech.*, **114**, 103112. https://doi.org/10.1016/j.compgeo.2019.103112.

Chen, S.L. and Abousleiman, Y.N. (2012), "Exact undrained elasto-plastic solution for cylindrical cavity expansion in modified cam clay soil mass", *Géotechnique,* **62**(5), 447-456. http://doi.org/10.1680/geot.11.P.027.

Chen, S.L. and Abousleiman, Y.N. (2013), "Exact drained solution for cylindrical cavity expansion in modified Cam Clay soil", *Géotechnique*, **63**(6), 510. https://doi.org/10.1680/geot.11.P.088.

Collins, I.F. and Yu, H.S. (1996), "Undrained cavity expansions in critical state soils", *Int. J. Numer. Anal. Meth. Geomech.*, **20**(7), 489-516. https://doi.org/10.1002/(SICI)1096-9853(199607)20:7<489::AID-NAG829>3.0.CO;2-V.

Einav, I. and Randolph, M.F. (2005), "Combining upper bound and strain path methods for evaluating penetration resistance", *Int. J. Numer. Meth. Eng.*, **63**(14), 1991-2016. https://doi.org/10.1002/nme.1350.

Gibson, R.E. and Anderson, W.F. (1961), "In situ measurement of soil properties with the pressure meter", *Civ. Eng. Public Works Rev.*, **56**, 615-618.

Hight, D.W., Bond, A.J. and Legge, J.D. (1992), "Characterization of the Bothkennaar clay: An overview", *Géotechnique*, **42**, 303-347. https://doi.org/10.1680/geot.1992.42.2.303.

Khanmohammadi, M. and Fakharian, K. (2018), "Evaluation of performance of piled-raft foundations on soft clay: A case study", *Geomech. Eng.*, **14**(1), 43-50. https://doi.org/10.12989/gae.2018.14.1.043.

Kwon, J., Kim, C., Im, J.C. and Yoo, J.W. (2018), "Effect of performance method of sand compaction piles on the mechanical behavior of reinforced soft clay", *Geomech. Eng.*, **14**(2), 175-185. https://doi.org/10.12989/gae.2018.14.2.175.

Li, C. and Zou, J.F. (2019), "Created cavity expansion solution in anisotropic and drained condition based on Cam-Clay model", *Geomech. Eng.*, **19**(2), 141-151. https://doi.org/10.12989/gae.2019.19.2.141.

Li, C., Zou, J.F. and Zhou, H. (2019b), "Cavity expansions in k0 consolidated clay", *Eur. J. Environ. Civ. Eng.*, 1-19. https://doi.org/10.1080/19648189.2019.1605937.

Li, L., Li, J., Sun, D.A. and Gong, W. (2017), "Unified solution to drained expansion of a spherical cavity in clay and sand", *Int. J. Geomech.*, **17**(8), 04017028. https://doi.org/10.1061/(ASCE)GM.1943-5622.0000909.

Liu, H., Zhou, H., Kong, G., Qin, H. and Zha, Y. (2017), "High pressure jet-grouting column installation effect in soft soil: Theoretical model and field application", *Comput. Geotech.*, **88**, 74-94. https://doi.org/10.1016/j.compgeo.2017.03.005.

Manandhar, S. and Yasufuku, N. (2012), "Analytical model for the end-bearing capacity of tapered piles using cavity expansion theory", *Adv. Civ. Eng.* https://doi.org/10.1155/2012/749540.

Manandhar, S. and Yasufuku, N. (2013), "Vertical bearing capacity of tapered piles in sands using cavity expansion theory", *Soils Found.*, **53**(6), 853-867. https://doi.org/10.1016/j.sandf.2013.10.005.

Manandhar, S., Yasufuku, N. and Omine, K. (2012), "Application of cavity expansion theory for evaluation of skin friction of tapered piles in sands", *Int. J. Geo-Eng.*, **4**(3), 5-17.

Merifield, R.S., Sloan, S.W. and Yu, H.S. (2001), "Stability of plate anchors in undrained clay", *Géotechnique*, **51**, 141-153. https://doi.org/10.1680/geot.2001.51.2.141.

Mo, P.Q. and Yu, H.S. (2017), "Undrained cavity expansion analysis with a unified state parameter model for clay and sand", *Géotechnique*, **67**(6), 503-515. https://doi.org/10.1680/jgeot.15.P.261.

Mo, P.Q., Marshall, A.M. and Yu, H.S. (2014), "Elastic-plastic solutions for expanding cavities embedded in two different cohesive-frictional materials", *Int. J. Numer. Meth. Eng.*, **38**, 961-977. https://doi.org/10.1002/nag.2288.

Mo, P.Q., Marshall, A.M. and Yu, H.S. (2017), "Interpretation of cone penetration test data in layered soils using cavity expansion analysis", *J. Geotech. Geoenviron. Eng.*, **143**, 04016084. https://doi.org/10.1061/(ASCE)GT.1943-5606.0001577.

Nash, D.F.T., Powell, J.J.M. and Lloyd, I.M. (1992), "Initial investigations of the soft clay test site at Bothkennar", *Géotechnique*, **42**, 163-181. https://doi.org/10.1680/geot.1992.42.2.163.

Qian, Z.H., Zou, J.F., Tian, J. and Pan, Q.J. (2020), "Estimations of active and passive earth thrusts of non-homogeneous frictional soils using a discretisation technique", *Comput. Geotech.*, **119**, 103366. https://doi.org/10.1016/j.compgeo.2019.103366.

Randolph, M.F., Carter, J.P. and Wroth, C.P. (1979), "Driven piles in clay-the effects of installation and subsequent consolidation", *Géotechnique*, **29**(4), 361-393. https://doi.org/10.1680/geot.1979.29.4.361.

Shuttle, D. (2007), "Cylindrical cavity expansion and contraction in Tresca soil", *Géotechnique*, **57**(3), 305-308. https://doi.org/10.1680/geot.2007.57.3.305.

Sivasithamparam, N. and Castro, J. (2020), "Undrained cylindrical cavity expansion in clays with fabric anisotropy and structure: Theoretical solution", *Comput. Geotech.*, **120**, 103386. https://doi.org/10.1016/j.compgeo.2019.103386.

Sivasithamparam, N. and Castro, J. (2018), "Undrained expansion of a cylindrical cavity in clays with fabric anisotropy: Theoretical solution", *Acta Geotechnica*, **13**(3), 729-746. https://doi.org/10.1007/s11440-017-0587-4.

Teh, C.I. and Houlsby, G.T. (1991), "Analytical study of the cone penetration test in clay", *Geotechnique*, **41**(1), 17-34. https://doi.org/10.1680/geot.1991.41.1.17.

Tian, P., Zhou, H. and Yin, F. (2018), "Elastic-perfectly plastic analytic solution for cylindrical cavity expansion considering rate-dependent effect and strength degradation of clay", *J. Central South Univ. Sci. Technol.*, **49**(6). https://doi.org/ 10.11817/j.issn.1672−7207.2018.06.024.

Vesic, A.S. (1972), "Expansion of cavities in infinite soil mass", *J. Soil Mech. Found. Div.*, **98**(3), 265-290.

Wang, S., Yin, S. and Wu, Z. (2012a), "Strain-softening analysis of a spherical cavity", *Int. J. Numer. Anal. Meth. Geomech.*, **36**(2), 182-202. https://doi.org/10.1002/nag.1002.

Wang, S., Yin, X., Tang, H. and Ge, X. (2012b), "A new approach for analyzing circular tunnel in strain-softening rock masses", *Int. J. Rock Mech. Min. Sci.*, **47**(1), 170-178.

Wijewickreme, D. and Weerasekara, L. (2015), "Analytical modeling of field axial pullout tests performed on buried extensible pipes", *Int. J. Geomech.*, **15**, 04014044. https://doi.org/10.1061/(ASCE)GM.1943-5622.0000388.

Xiao, Y. and Liu, H. (2016a), "Elastoplastic constitutive model for rockfill materials considering particle breakage", *Int. J. Geomech.*, **17**(1), 04016041. https://doi.org/10.1061/(ASCE)GM.1943-5622.0000388.

Xiao, Y., Liu, H., Ding, X., Chen, Y., Jiang, J. and Zhang, W. (2016b), "Influence of particle breakage on critical state line of rockfill material", *Int. J. Geomech.*, **16**(1), 04015031. https://doi.org/10.1061/(ASCE)GM.1943-5622.0000538.

Yu, H.S. and Carter, J.P. (2002), "Rigorous similarity solutions for cavity expansion in cohesive-frictional soils", *Int. J. Geomech.*, **2**(2), 233-258. https://doi.org/10.1061/(ASCE)1532-3641(2002)2:2(233).

Yu, H.S. and Houlsby, G.T. (1991), "Finite cavity expansion in dilatant soils: loading analysis", *Géotechnique*, **42**(4), 649-654. https://doi.org/10.1680/geot.1991.41.2.173.

Yu, H.S. and Rowe, R.K. (1999), "Plasticity solutions for soil behaviour around contracting cavities and tunnels", *Int. J. Numer. Anal. Meth. Geomech.*, **23**, 1245-1279. https://doi.org/10.1002/(SICI)1096-9853(199910)23:12<1245::AID-NAG30>3.0.CO;2-W.

Zhang, J. and Li, L. (2020), "Similarity solution for undrained cylindrical cavity contraction in anisotropic modified Cam-clay model soils", *Comput. Geotech.*, **120**, 103405. https://doi.org/10.1016/j.compgeo.2019.103405.

Zhou, H. and Randolph, M.F. (2007), "Computational techniques and shear band development for cylindrical and spherical penetrometers in strain-softening clay", *Int. J. Geomech.*, **7**(4), 287-295. https://doi.org/10.1061/(ASCE)1532-3641(2007)7:4(287).

Zhou, H., Kong, G., Liu, H. and Laloui, L. (2018), "Similarity solution for cavity expansion in thermoplastic soil", *Int. J. Numer. Anal. Meth. Geomech.*, **42**(2), 274-294. https://doi.org/10.1002/nag.2724.

Zou, J.F. and Xia, Z.Q. (2017), "Closed-form solution for cavity expansion in strain-softening and undrained soil mass based on the unified strength failure criterion", *Int. J. Geomech.*, **17**(9), 04017046. https://doi.org/10.1061/(ASCE)GM.1943-5622.0000927.

Zou, J.F., Chen, K.F. and Pan, Q.J. (2017), "Influences of seepage force and out-of-plane stress on cavity contracting and tunnel opening", *Geomech. Eng.*, **13**(6), 907-928. https://doi.org/10.12989/gae.2017.13.6.907.

Zou, J.F., Xia, Z.Q. and Dan, H.C. (2016), "Theoretical solutions for displacement and stress of a circular opening reinforced by grouted rock bolt", *Geomech. Eng.*, **11**(3), 439-455. https://doi.org/10.12989/gae.2016.11.3.439.